Earth Syst. Dynam. Discuss., https://doi.org/10.5194/esd-2018-78
Manuscript under review for journal Earth Syst. Dynam.
Discussion started: 3 December 2018
© Author(s) 2018. CC BY 4.0 License.

Earth System Dynamics
Discussions
Open Access
EGU

MAXIMUM POWER OF SALINE AND FRESH WATER MIXING IN ESTUARIES

Zhilin Zhang[1] and Hubert Savenije[1]

[1]Department of Water Management, Delft University of Technology, Delft, the Netherlands.

Correspondence: Hubert Savenije (h.h.g.savenije@tudelft.nl)

Abstract. Natural systems evolve towards a state of maximum power (*Kleidon*, 2016), leading to higher levels of entropy production by different mechanisms, including the gravitational circulation in alluvial estuaries. Gravitational circulation is driven by the potential energy of the fresh water. Due to the density difference between seawater and riverwater, the water level on the river side is higher. The hydrostatic forces on both sides are equal, but have different working lines. This triggers an (accelerating) angular moment, providing rotational kinetic energy into the system, part of which drives mixing by gravitational circulation mixing; the remainder is transferred into dissipated energy by friction while mixing. With a constant discharge over a tidal cycle, the density-driven gravitational circulation in the estuarine system performs work at maximum power, lifting up saline water and bringing down fresh water against gravity. The rotational flow causes the spread of salinity, which is mathematically represented by the dispersion coefficient. Accordingly, a new equation for the dispersion coefficient due to the density-driven mechanism has been derived. Together with the steady state advection-dispersion equation, this resulted in a new analytical model for gravitational salinity intrusion. The simulated longitudinal salinity profiles have been confronted with observations in a myriad of estuaries worldwide. It shows that the performance is promising in eighteen out of twenty-three estuaries, with relatively large convergence length. Finally, a predictive equation is presented for the dispersion coefficient at the boundary. Overall, the maximum power concept has provided an alternative for describing the dispersion coefficient due to gravitational circulation in alluvial estuaries.

1 Introduction

Estuaries are water bodies where rivers with fresh water meet the open sea. The longitudinal salinity difference causes a water level gradient along the estuary. Hence, the hydrostatic forces from seaside and riverside have different working lines, which trigger an angular moment and drive gravitational circulation (*Savenije*, 2005). This density-driven gravitational circulation is one of the most significant mixing mechanisms in alluvial estuaries (another is tide-driven mixing mechanism) (*Fischer et al.*, 1979). *Kleidon* (2016) described the concept of maximum power in the Earth system, implying that freely evolving systems perform work and dissipate energy at maximum power (close to or at the Carnot limit). Using this concept, gravitational circulation is assumed to take place at the maximum power limit. Earlier, the maximum power concept was used to solve the saline and fresh water mixing as in thermodynamic equilibrium system (*Zhang and Savenije*, 2018). However, this effort was

Earth Syst. Dynam. Discuss., https://doi.org/10.5194/esd-2018-78
Manuscript under review for journal Earth Syst. Dynam.
Discussion started: 3 December 2018
© Author(s) 2018. CC BY 4.0 License.

not fully successful, probably because that the freshwater discharge provides continuous potential energy into the estuary so that the system is not isolated.

Kleidon (2016) presented an example of the maximum power limit for non-thermal energy conversions. In the example, a fluid is kept in motion by an accelerating force which provides kinetic energy to the system. The velocity of the fluid is slowed down by friction and the remainder is converted into another form of energy. If the velocity is too large, the friction is large and energy dissipation dominates, then the power of the force to generate work is limited. In contrast, if the velocity is too small, the power is not enough to generate work. Hence, there is an optimum value for the product of the force and velocity to produce maximum useful energy.

Estuaries are comparable to this system. This article tries to solve the dynamics of an estuary using a similar concept considering it as an open system.

2 Moment balance for an open estuary system

In an estuary, the cross-sectional average hydrostatic forces have equal values along the estuary axis. Over a segment, the forces are opposed but working on different lines of action due to the density gradient in upstream and downstream directions. As a result, they exert an angular moment M_{acc} that drives the gravitational circulation, performing as accelerating energy. N_{fric} is the energy dissipation due to friction. The remainder moment M_{ex} drives the dispersive movement and performs work (Figure 1). Hence, the balance in steady state in a segment is

$$M_{\mathrm{acc}} - M_{\mathrm{ex}} - N_{\mathrm{fric}} = 0 \ . \tag{1}$$

Energy dissipation is expressed as

$$N_{\mathrm{fric}} = F_{\mathrm{fric}} l_m \ , \tag{2}$$

with F_{fric} being the friction that causes energy dissipation in N and l_m the dispersive distance scale where energy dissipates in m.

Friction is expressed as

$$F_{\mathrm{fric}} = \tau O \ , \tag{3}$$

where τ is the shear stress in $\mathrm{kgm^{-1}s^{-2}}$ and O is the contact area in $\mathrm{m^2}$. Gravitational circulation has two length scales: a vertical and a horizontal one. The horizontal length scale of the circulation is the tidal excursion E, which is the distance a water particle travels on the tide; the vertical length scale is the depth h, over which saline water is moved upward to the surface, and over which relatively fresh water is moved downward to the bottom. Since the process of gravitational mixing is essentially to move the saline water up and the fresher water down vertically, the contact area for the resistance against this movement is determined by the depth (h) and the width (B). Following that reasoning, O is assumed equal to $2Bh$, one Bh for the upward lift of saline water and one Bh for the downward push of relatively fresh water. The dispersive distance then equals two times the depth ($l_m = 2h$).

Earth Syst. Dynam. Discuss., https://doi.org/10.5194/esd-2018-78
Manuscript under review for journal Earth Syst. Dynam.
Discussion started: 3 December 2018
© Author(s) 2018. CC BY 4.0 License.

Earth System Dynamics Discussions
Open Access
EGU

2.1 Maximum power condition in estuaries

Because the velocity of the dispersive gravitational circulation is small, the mixing flow is assumed to be laminar. The shear stress is typically a function of flow velocity (v): $\tau = \rho q v$, with ρ being the density in $\mathrm{kgm^{-3}}$ and q being a laminar resistance in $\mathrm{ms^{-1}}$. The latter is assumed to be proportional to the tidal velocity amplitude ($q \propto E/T$), where T is the tidal period in s. Hence, the flow velocity representing the gravitational circulation is:

$$v = \frac{M_{\mathrm{acc}} - M_{\mathrm{ex}}}{4\rho q B h^2} \, . \tag{4}$$

Power is defined by the product of a force and its velocity. The power of torque (angular moment) is defined as the product of the moment and its angular velocity. Hence, the power is defined as

$$P = M_{\mathrm{ex}}\omega = M_{\mathrm{ex}} \frac{v}{h/2} 2\pi = \frac{2\pi}{\rho q B h^3} \left(M_{\mathrm{acc}} - M_{\mathrm{ex}}\right) M_{\mathrm{ex}} \, , \tag{5}$$

where ω is the angular velocity or the rotational speed in $\mathrm{s^{-1}}$. Figure 2 illustrates how the execution moment and the flow velocity vary. If the working moment is too large and causes fast mixing flow, the energy dissipation is large and diminishes the flow velocity. If it is too small, the mixing would also be sub-optional. In analogy with *Kleidon* (2016), the product of the working moment and the flow velocity has a well-defined maximum. The maximum power (MP) is then obtained by: $\partial P / \partial M_{\mathrm{ex}} = 0$. Hence, the optimum values of the execution moment $M_{\mathrm{ex,opt}}$ and the flow velocity v_{opt} are

$$M_{\mathrm{ex,opt}} = \frac{1}{2} M_{\mathrm{acc}} \tag{6}$$

and

$$v_{\mathrm{opt}} = \frac{M_{\mathrm{acc}}}{8\rho q B h^2} \, . \tag{7}$$

Here, the accelerating force (F_{acc}) that produces the angular moment is the hydrostatic force obtained by integrating the hydraulic pressure over the depth:

$$F_{\mathrm{acc}} = \frac{1}{2} \rho_0 g h^2 B \, , \tag{8}$$

where ρ_0 is the density of the seaside in $\mathrm{kgm^{-3}}$.

The accelerating moment has an arm $\Delta h/3$ (*Savenije*, 2005). The water level gradient according to the balance of the hydrostatic pressures results in:

$$\frac{\mathrm{d}h}{\mathrm{d}x} = -\frac{h}{2\rho} \frac{\mathrm{d}\rho}{\mathrm{d}x} \, , \tag{9}$$

where x is the distance in m. Density is a function of salinity (S): $\rho = \rho_f (1 + c_S S)$, where ρ_f is the density of the freshwater in $\mathrm{kgm^{-3}}$ and c_S ($\approx 7.8 \times 10^{-4}$) is the saline expansivity in $\mathrm{psu^{-1}}$.

Subsequently, the accelerating moment drives gravitational circulation that can be described as:

$$M_{\mathrm{acc}} = F_{\mathrm{acc}} \frac{1}{3} \frac{\mathrm{d}h}{\mathrm{d}x} E = -\frac{1}{12} \rho_0 g h^3 B c_S \frac{\mathrm{d}S}{\mathrm{d}x} E \, , \tag{10}$$

Earth Syst. Dynam. Discuss., https://doi.org/10.5194/esd-2018-78
Manuscript under review for journal Earth Syst. Dynam.
Discussion started: 3 December 2018
© Author(s) 2018. CC BY 4.0 License.

Earth System Dynamics Discussions Open Access EGU

where E is the horizontal length scale of the gravitational circulation in m.

In steady state, the one-dimensional advection-dispersion equation averaged over the cross section and over a tidal cycle reads:

$$|Q|S + AD\frac{\mathrm{d}S}{\mathrm{d}x} = 0\,, \tag{11}$$

where Q is the freshwater discharge in $\mathrm{m^3\,s^{-1}}$, A is the cross-sectional area in $\mathrm{m^2}$, and D is the dispersion coefficient in $\mathrm{m^2\,s^{-1}}$. The positive direction of flow is in the upstream direction.

Accordingly, the optimum velocity is

$$v_{\mathrm{opt}} \propto \frac{c_S g h T}{96}\frac{|Q|S}{AD}\,. \tag{12}$$

Assuming that the steady state over a tidal cycle is driven mainly by the accelerating moment especially in the upstream part where tidal effects are small and this gravitational circulation (D_g) is proportional to the dispersive residual velocity ($D_g \propto vE$),

$$D_g \propto \left(\frac{c_S g}{96}\frac{S|Q|ET}{B}\right)^{1/2}\,. \tag{13}$$

This equation indicates that the dimensionless dispersion coefficient is proportional to the root of the estuarine Richardson number N_R:

$$\frac{D_g}{vE} \propto {N_R}^{0.5} = \left(c_S S\frac{gh}{v^2}\frac{|Q|T}{AE}\right)^{0.5}\,, \tag{14}$$

where v is the tidal velocity amplitude in $\mathrm{m\,s^{-1}}$. The Richardson number describes the balance between the potential energy of the fresh water flowing into the estuary ($\rho g h|Q|T/2$) and the kinetic energy of the tidal flood flow ($\rho v^2 AE/2$) (*Fischer et al.*, 1979; *Savenije*, 2005; *Zhang and Savenije*, 2017).

2.1.1 Analytical solution for the dispersion equation

Equations derived from the maximum power concept are obtained along the estuary axis, hence they can be used at any segment along the estuary. Then, equation (13) becomes

$$D_g(x) = C_3\left(\frac{S|Q|ET}{B}\right)^{1/2}\,, \tag{15}$$

where C_3 is a factor in $\mathrm{psu^{-1}ms^{-2}}$ and all local variables are a function of x.

The following equations are used for the tidal excursion and width in alluvial estuaries:

$$E(x) = E_0 \mathrm{e}^{\delta_H (x - x_1)}\,, \tag{16}$$

$$B(x) = B_0 \mathrm{e}^{-(x - x_1)/b}\,, \tag{17}$$

Earth Syst. Dynam. Discuss., https://doi.org/10.5194/esd-2018-78
Manuscript under review for journal Earth Syst. Dynam.
Discussion started: 3 December 2018
© Author(s) 2018. CC BY 4.0 License.

Earth System Dynamics Discussions Open Access EGU

where δ_H is the tidal damping rate in m^{-1} and b is the geometric convergence length of the width in m. The subscript '0' represents parameters at the boundary condition ($x = x_1$).

At the boundary, equation (15) is given by:

$$D_{g0} = C_3 \left(\frac{S_0 |Q| E_0}{{B_0}^2} \right)^{1/2} . \tag{18}$$

Substitution of equations (16)–(18) into (15) gives

$$D_g(x) = D_{g0} \left(\frac{S}{S_0} \right)^{1/2} e^{\Omega(x-x_1)} , \tag{19}$$

with $\Omega = \delta_H/2 + 1/(2b)$.

Differentiating D_g with respect to x and using the steady state equation (11) results in

$$\frac{\mathrm{d}D_g}{\mathrm{d}x} = \frac{D_g}{2S}\frac{\mathrm{d}S}{\mathrm{d}x} + \Omega D_g = \Omega D_g - \frac{1}{2}\frac{|Q|}{A} . \tag{20}$$

The cross-sectional area A is given by

$$A(x) = A_0 \mathrm{e}^{-(x-x_1)/a} , \tag{21}$$

where a is the convergence length of the cross section in m.

Substituting equation (21) into (20) and in analogy with *Kuijper and Van Rijn* (2011) and *Zhang and Savenije* (2017), the solution of the linear differential equation (20) is

$$\frac{D_g}{D_{g0}} = e^{\Omega(x-x_1)} - \frac{|Q|\zeta}{2A_0 D_{g0}} \left[e^{(x-x_1)/a} - e^{\Omega(x-x_1)} \right] , \tag{22}$$

with $\zeta = a/(1-\Omega a)$.

At the salinity intrusion limit ($x = L$), $D_g = 0$, resulting in

$$L = \zeta \ln \left(1 + \frac{2A_0 D_{g0}}{|Q|\zeta} \right) + x_1 . \tag{23}$$

The solution for the longitudinal salinity distribution yields

$$\frac{S}{S_0} = \left\{ 1 - \frac{|Q|\zeta}{2A_0 D_{g0}} \left[e^{(x-x_1)/\zeta} - 1 \right] \right\}^2 , \tag{24}$$

This solution is comparable to other research. It is similar with *Savenije* (2005) if $\Omega = 0$, while his solutions has an empirical Van der Burgh coefficient K. Besides, the solution is the same as *Kuijper and Van Rijn* (2011) if a equals b, which implies that the depth is constant along the estuary.

With these new analytical equations, the dispersion and salinity distribution can be obtained, using the boundary conditions (D_0 and S_0).

Earth Syst. Dynam. Discuss., https://doi.org/10.5194/esd-2018-78
Manuscript under review for journal Earth Syst. Dynam.
Discussion started: 3 December 2018
© Author(s) 2018. CC BY 4.0 License.

Earth System Dynamics Discussions Open Access EGU

3 Empirical validation and discussion

The boundary condition is often taken at the geometric inflection point ($x = x_1$) if the estuary has one. The compilation of the Muar estuary in Figure 3 is an example. Vertical dash lines displays the inflection point. If there is no inflection point such as the Landak estuary, the boundary condition is taken at the estuary mouth ($x = 0$). Figure 3 demonstrates that the geometry of the alluvial estuaries fits well on semi-logarithmic paper, supporting the exponential functions of the cross section and the width (equations (16) and (21)).

Subsequently, equation (24) is used by confronting the solution with observations, using selected boundary conditions. Appendix B shows how the new equation based on the maximum power concept works in twenty-three estuaries around the world. The Van der Burgh (VDB) method (*Savenije*, 2005) (which is proved performing well in different parts of the world and includes all mixing mechanisms) is used for comparison. Density-driven gravitational circulation is one part of the dispersive actions in estuaries. Hence, the total dispersive process from the Van der Burgh method (D_{VDB}) must be larger than the dispersion from the maximum power method (D_{MP}). The general geometry and measurements follow the database from *Savenije* (2012), *Gisen* (2015), and *Zhang and Savenije* (2017). The information of the VDB and MP methods is summarized in Table **??**. The measurement date chosen from each estuary with star-marked label is used (in Appendix B).

It shows that the simulation curves by the new MP method are in recession shape, increasing seaward from the inflection point owing to the widening. However, the salinity observations can be simulated well landward from the inflection point in most estuaries. In the Bernam, the Pangani, the Rembau Linggi, and the Incomati estuaries, the part in the center, where D_{MP} closely approach D_{VDB}, fits well. In these estuaries, the calibration is slightly lower than the measurement near the intrusion limit. In general, the dispersion from the maximum power method declines upstream the inflection point approximately with the total dispersion from the empirical Van der Burgh method, which means that the gravitational circulation is the predominant mixing mechanism in the landward part of these estuaries.

However, in the Thames (#8), the Delaware (#20), the Scheldt (#21), and the Pungwe (#22), the new approach seems not to work, both from the salinity and dispersion profiles. Figure 4 shows the relation between the geometry and the K values. It can be seen that estuaries with poor performances by MP approach have lower b/B_0 and K values. The former is therefore an effective dimensionless parameter representing the geometry. However, not all estuaries with strong convergent geometry perform poor, revealing that the geometry is not the only effect. According to the expression of Ω_2, tidal damping can play a role. In wide estuaries with strong convergence, the role of gravitational circulation is insufficient to describe the mixing. Tidal mixing processes such as lateral circulation, tidal pumping, and tidal shear are dominant. The Scheldt with preferential ebb and flood channels is a case in point (*Nguyen et al.*, 2008). Besides, the Corantijn (#9) is considered uncertain because it has a low b/B_0 value and contains few observations.

Overall, the maximum power approach in open systems is a useful tool to understand the mixing processes in most estuaries. In the upstream part where the effect of the tide is small, gravitational circulation plays the main role. Meanwhile, observations upstream are more important for salinity intrusion research and more relevant for water users. Where the salinity is high, it is less relevant since the water is already too saline to use.

Earth Syst. Dynam. Discuss., https://doi.org/10.5194/esd-2018-78
Manuscript under review for journal Earth Syst. Dynam.
Discussion started: 3 December 2018
© Author(s) 2018. CC BY 4.0 License.

This study provides an approach to define the dispersion coefficient which is proportional to the product of the velocity of the flow due to the gravitational circulation and the tidal excursion length. The dispersive velocity actually represents the ability of the density-driven mechanism. Based on the maximum power method (equation (15)), the velocity can be described as

$$v \propto \left(\frac{c_S S g h}{96} \frac{|Q|T}{AE} \right)^{1/2} . \tag{25}$$

Here, the dispersive flow due to gravitational circulation strengthens with larger freshwater discharge (more stratification) and weakens with stronger tide (less stratification).

Using the calibrated dispersion coefficient at the inflection point, C_3 can be calculated. Except in estuaries with poor performance, C_3 values range from 3.5×10^{-3} to 10.0×10^{-3} with an average 6.8×10^{-3} (the relative standard derivation equals 0.26). Using the average C_3 value to predict D_{g0} (equation (15)), Figure 5 shows how the predictive equation performs. It reveals that almost all the data falls within a factor of 2, and the maximum power method underestimates the dispersion coefficient in estuaries with low b/B_0 values (in red). Finally, R^2 value of the regression in Figure 5 equals 0.86. Considering all the uncertainties in the measurement, C_3 equalling 6.8×10^{-3} is a promising approximation to predict D_{g0}.

In addition, the time needed to achieve the optimum situation is not sure (larger or less than a tidal period). In a low flow situation (which is the critical circumstance for salt intrusion) the variation of the river discharge is slow (following an exponential decline). If the time scale of flow recession is large compared to the time scale of salinity intrusion then it is reasonable to assume that maximum power optimum is achieved based on the steady-state assumption. The uncertainty in measurement can lead to outliers.

4 Conclusions

An estuary is an open system which has a maximum power limit when the accelerating source is stable. This study has described a moment balance approach to non-thermal open systems, yielding a new equation (15) for the dispersion coefficient due to the density-driven gravitational circulation. It shows that the dispersive action is closely related to the salinity, the freshwater discharge, the tide, and the estuarine width. This equation has been used to solve the tidal average salinity and dispersion distributions together with the steady-state equation (11). The maximum power model has then been validated with fifty salinity observations in twenty-three estuaries worldwide and compared with the Van der Burgh method. Generally, the new equation is a helpful tool to analysis the estuaries, providing an alternative solution for the empirical Van der Burgh method where the gravitational circulation is the dominant mixing mechanism. A predictive equation for dispersion at the boundary has also been provided.

As can be seen in Appendix B, the gravitational dispersion is always smaller than the total effective dispersion obtained by the Van der Burgh method. In all estuaries that have a wide mouth, we see substantial tide-driven dispersion, most probably as a result of interacting preferential ebb and flood channels. This tide-driven mechanism is responsible for the (sometimes pronounced) concave slope of the salinity curve near the mouth. In the middle reach where the salinity gradient is steepest, the density-driven dispersion is all dominant and the density-driven dispersion equals the total effective dispersion. Further up-

Earth Syst. Dynam. Discuss., https://doi.org/10.5194/esd-2018-78
Manuscript under review for journal Earth Syst. Dynam.
Discussion started: 3 December 2018
© Author(s) 2018. CC BY 4.0 License.

stream, where the salinity gradient gradually tends to zero and the estuary becomes narrower, we see the tide-driven circulation again becoming more prominent. This is in the part of the estuary where the width to depth ratio becomes smaller and the bank shear results in more pronounced lateral velocity gradients and hence more pronounced lateral circulation. This tide-driven mixing mechanism is particularly strong in macro-tidal estuaries such as the Thames, Scheldt, Pungue, and Delaware.

This study is a further development of the paper by *Zhang and Savenije* (2018), in which estuaries were considered as isolated systems (to achieve thermodynamic equilibrium). More reliable observations in other estuaries are suggested to validate this maximum power method.

Data availability. About the data, all observations are available on the website at https://salinityandtides.com/.

Appendix A: Notation

Table A1. Notations for symbols used regularly.

Symbol	Meaning	Dimension	Symbol	Meaning	Dimension
a	cross-sectional convergence length	[L]	M	moment	$[\mathrm{ML^2T^{-2}}]$
A	cross-sectional area	$[\mathrm{L^2}]$	N_R	estuarine Richardson number	[-]
b	width convergence length	[L]	O	contact area	$[\mathrm{L^2}]$
B	width	[L]	P	Power	$[\mathrm{ML^2T^{-3}}]$
c_s	saline expansivety	$[\mathrm{psu^{-1}}]$	q	laminar resistance	$[\mathrm{LT^{-1}}]$
D	dispersion coefficient	$[\mathrm{L^2T^{-1}}]$	Q	freshwater discharge	$[\mathrm{L^3T^{-1}}]$
D_g	dispersion due to gravitational circulation	$[\mathrm{L^2T^{-1}}]$	S	salinity	[psu]
E	tidal excursion length	[L]	T	tidal period	[T]
F	force	$[\mathrm{MLT^{-2}}]$	v	velocity of dispersive movement	$[\mathrm{LT^{-1}}]$
g	gravity acceleration	$[\mathrm{LT^{-2}}]$	δ_H	damping/amplifying rate	$[\mathrm{L^{-1}}]$
h	depth	[L]	ρ	density of water	$[\mathrm{ML^{-3}}]$
K	Van der Burgh's coefficient	[-]	τ	shear stress	$[\mathrm{ML^{-1}T^{-2}}]$
l_m	dispersive distance	[L]	v	tidal velocity amplitude	$[\mathrm{LT^{-1}}]$
L	intrusion length	[L]			

Earth Syst. Dynam. Discuss., https://doi.org/10.5194/esd-2018-78
Manuscript under review for journal Earth Syst. Dynam.
Discussion started: 3 December 2018
© Author(s) 2018. CC BY 4.0 License.

Earth System Dynamics Discussions
Open Access
EGU

Appendix B: Application of the maximum power method

This appendix represents the application in twenty-three estuaries around the world of the maximum power method for determining the dispersion coefficient and the salinity distribution using equations (22) and (24), compared to salinity observations. The empirical Van der Burgh method is included as reference.

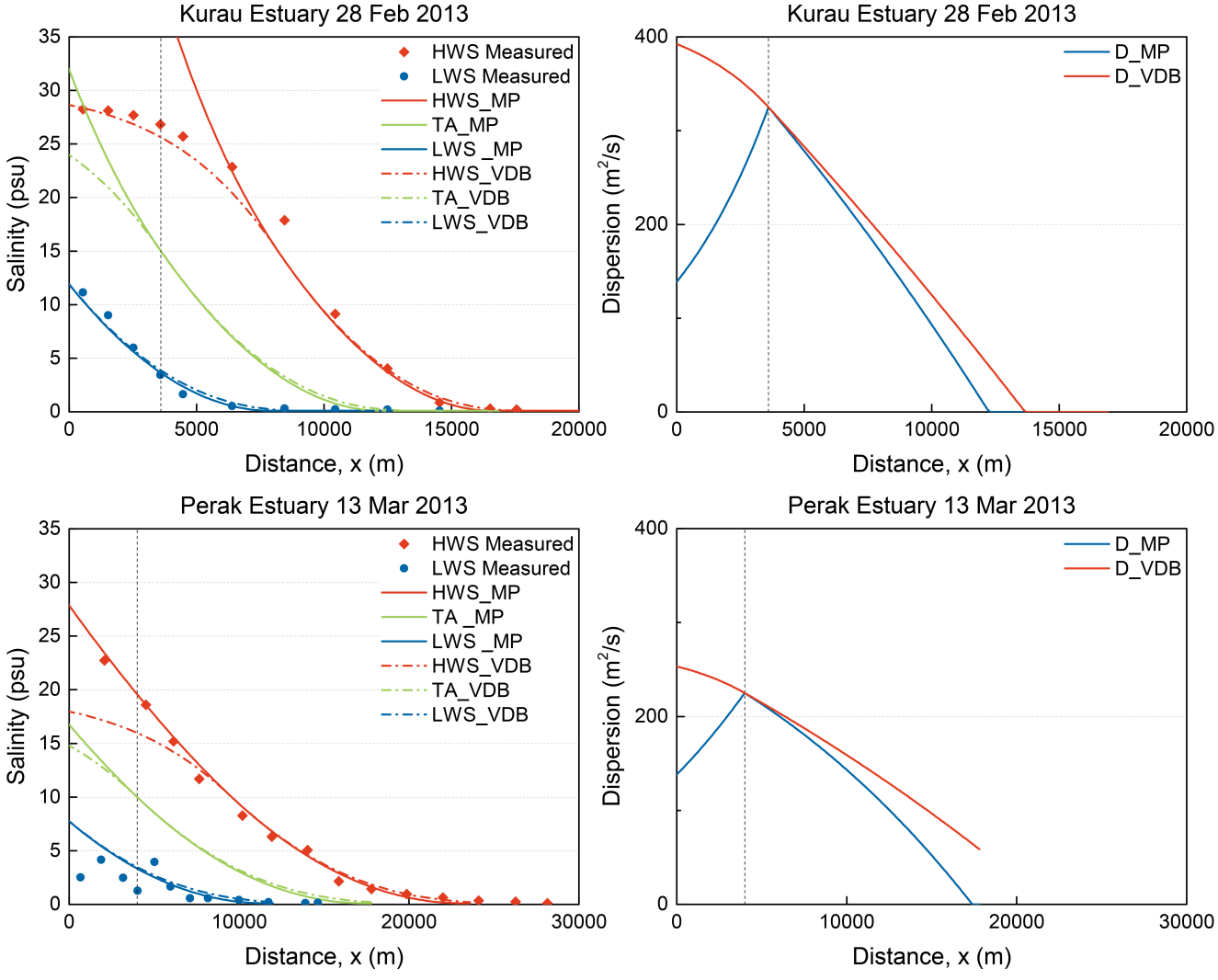

Earth Syst. Dynam. Discuss., https://doi.org/10.5194/esd-2018-78
Manuscript under review for journal Earth Syst. Dynam.
Discussion started: 3 December 2018
© Author(s) 2018. CC BY 4.0 License.

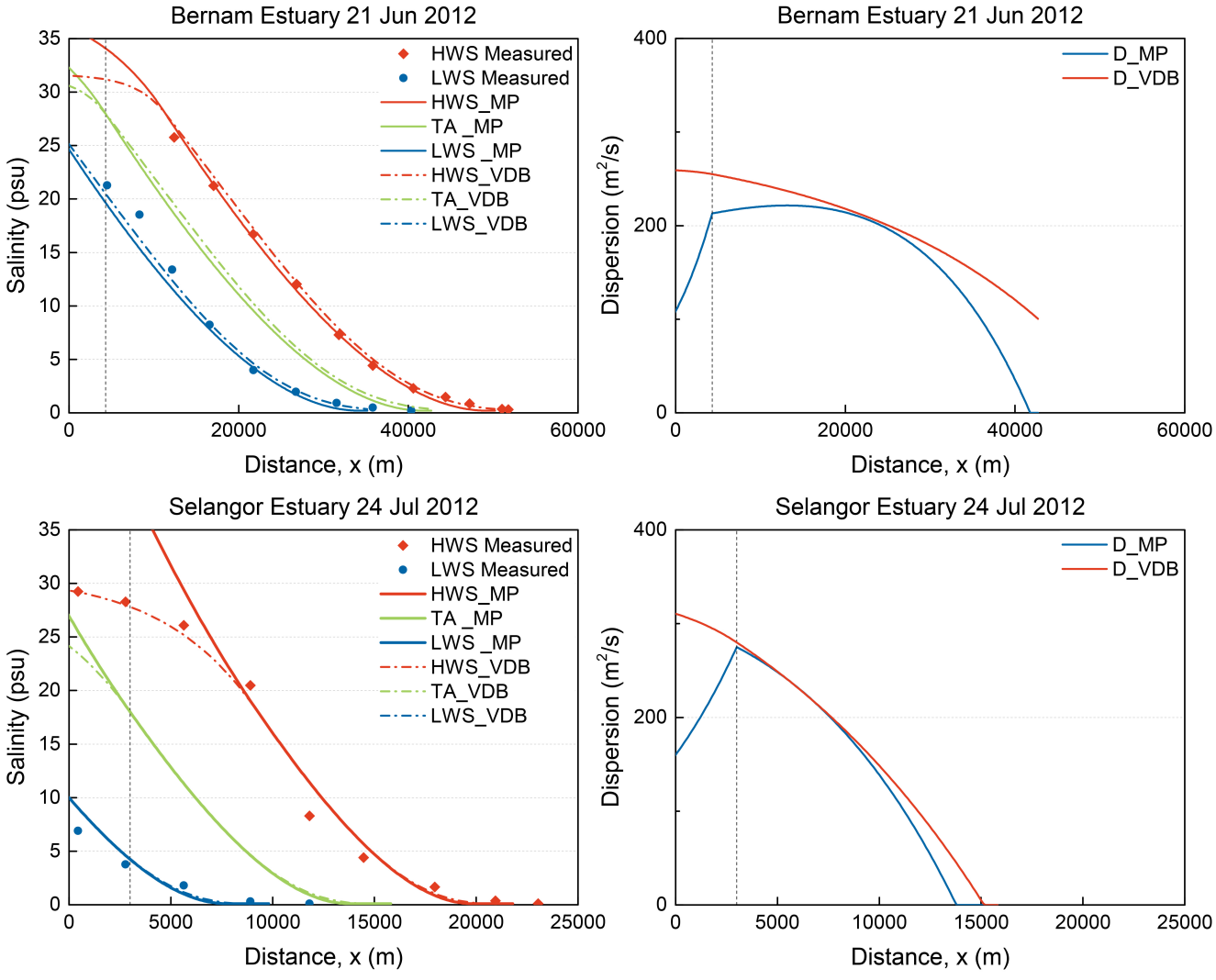

Earth Syst. Dynam. Discuss., https://doi.org/10.5194/esd-2018-78
Manuscript under review for journal Earth Syst. Dynam.
Discussion started: 3 December 2018
© Author(s) 2018. CC BY 4.0 License.

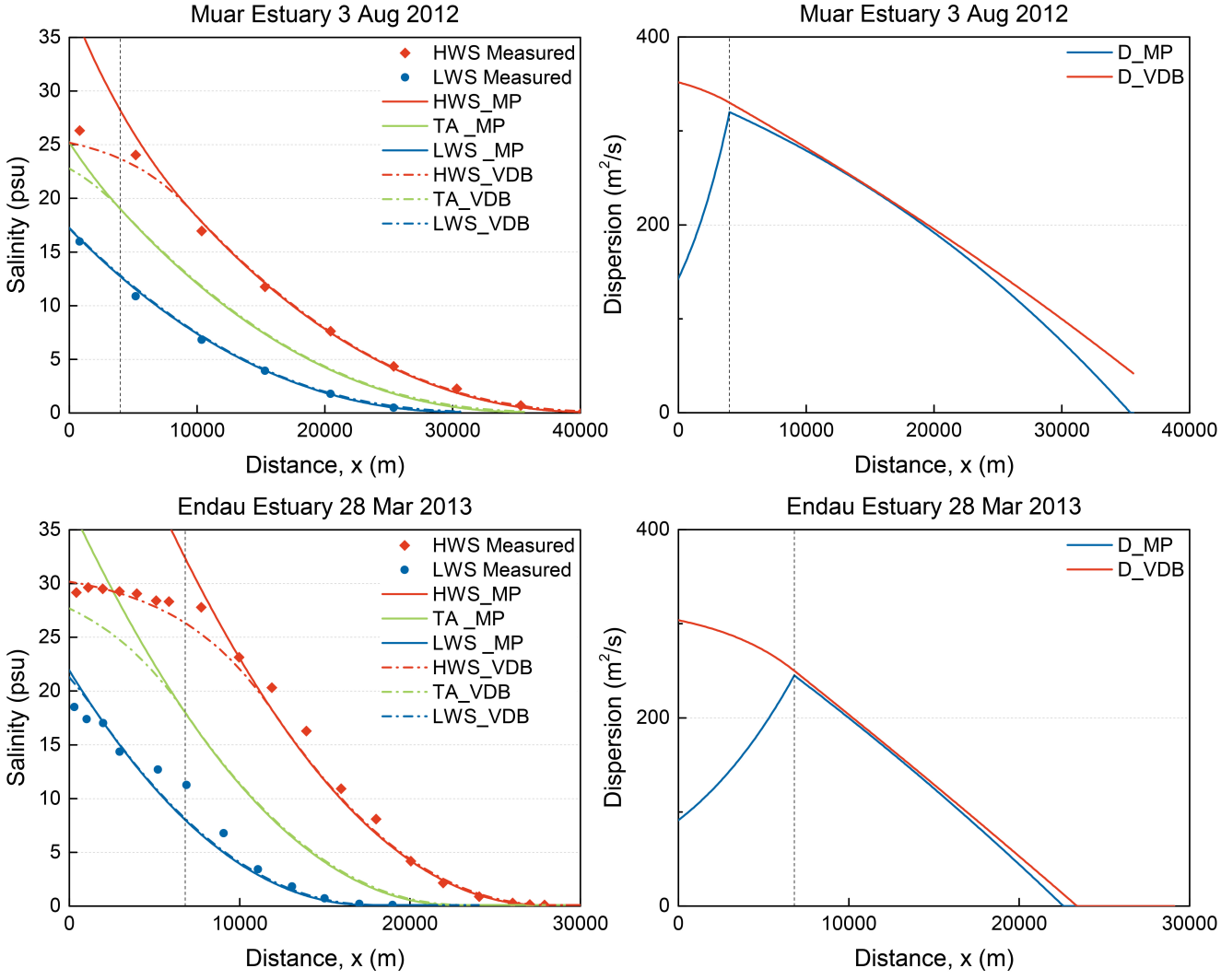

Earth Syst. Dynam. Discuss., https://doi.org/10.5194/esd-2018-78
Manuscript under review for journal Earth Syst. Dynam.
Discussion started: 3 December 2018
© Author(s) 2018. CC BY 4.0 License.

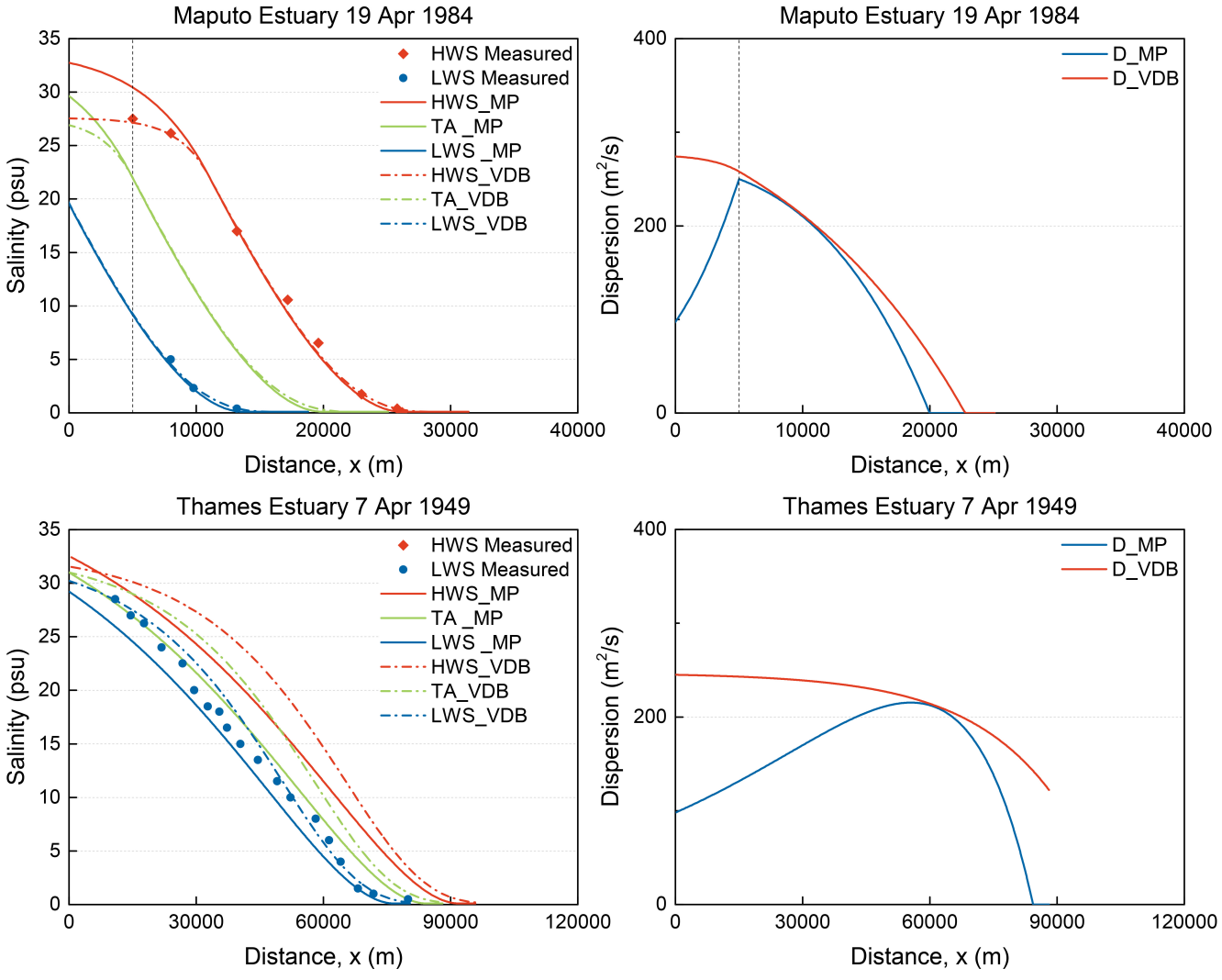

Earth Syst. Dynam. Discuss., https://doi.org/10.5194/esd-2018-78
Manuscript under review for journal Earth Syst. Dynam.
Discussion started: 3 December 2018
© Author(s) 2018. CC BY 4.0 License.

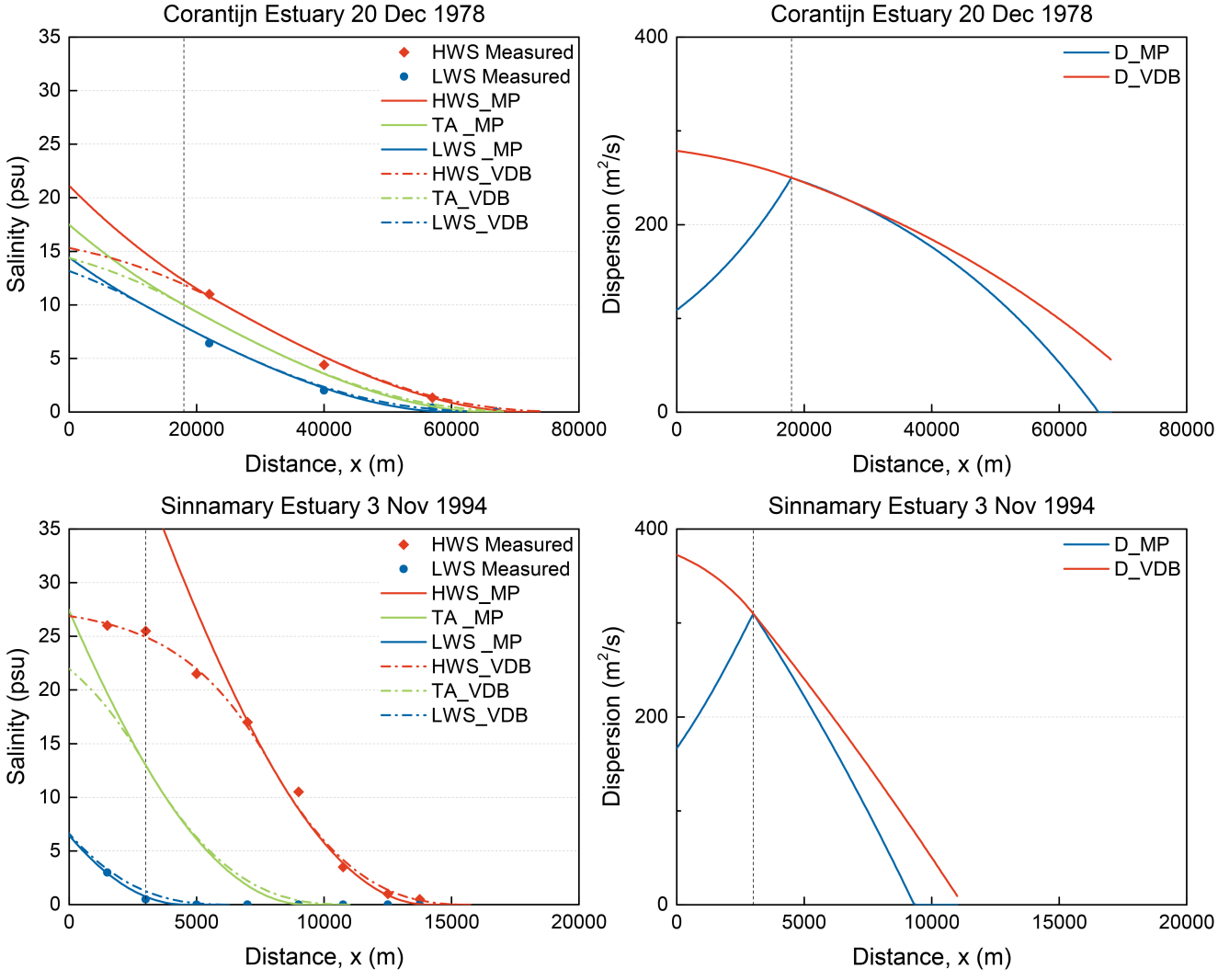

Earth Syst. Dynam. Discuss., https://doi.org/10.5194/esd-2018-78
Manuscript under review for journal Earth Syst. Dynam.
Discussion started: 3 December 2018
© Author(s) 2018. CC BY 4.0 License.

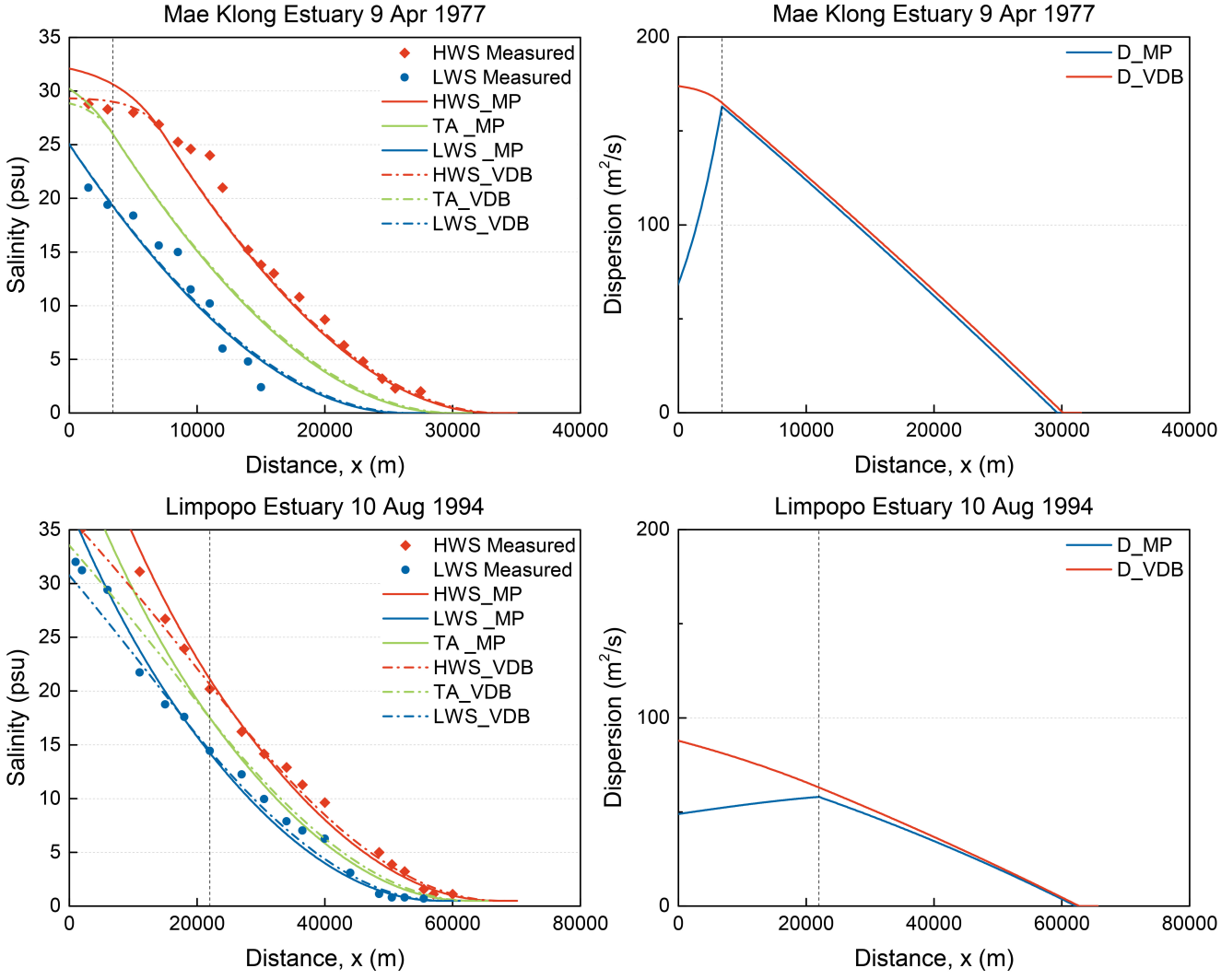

Earth Syst. Dynam. Discuss., https://doi.org/10.5194/esd-2018-78
Manuscript under review for journal Earth Syst. Dynam.
Discussion started: 3 December 2018
© Author(s) 2018. CC BY 4.0 License.

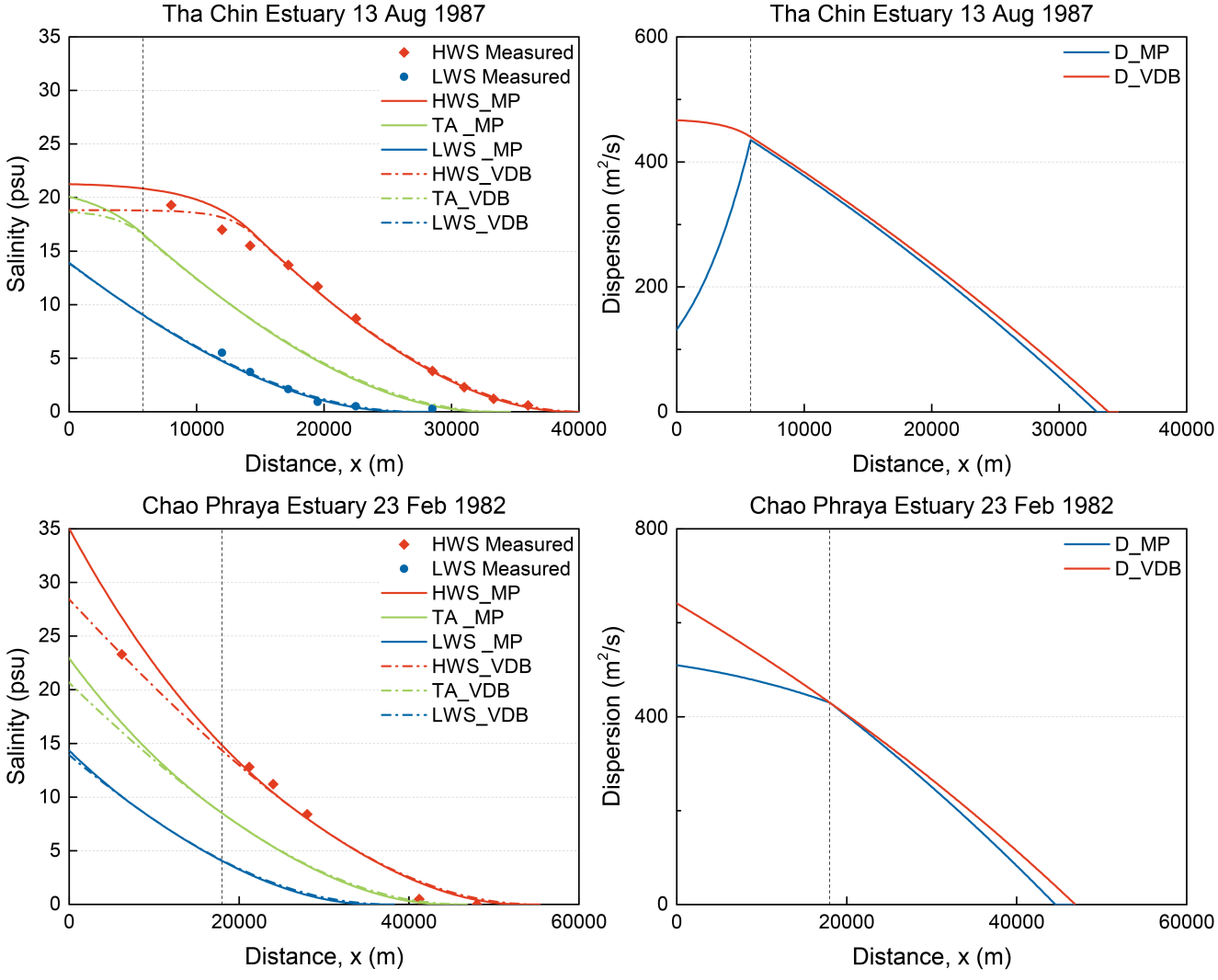

Earth Syst. Dynam. Discuss., https://doi.org/10.5194/esd-2018-78
Manuscript under review for journal Earth Syst. Dynam.
Discussion started: 3 December 2018
© Author(s) 2018. CC BY 4.0 License.

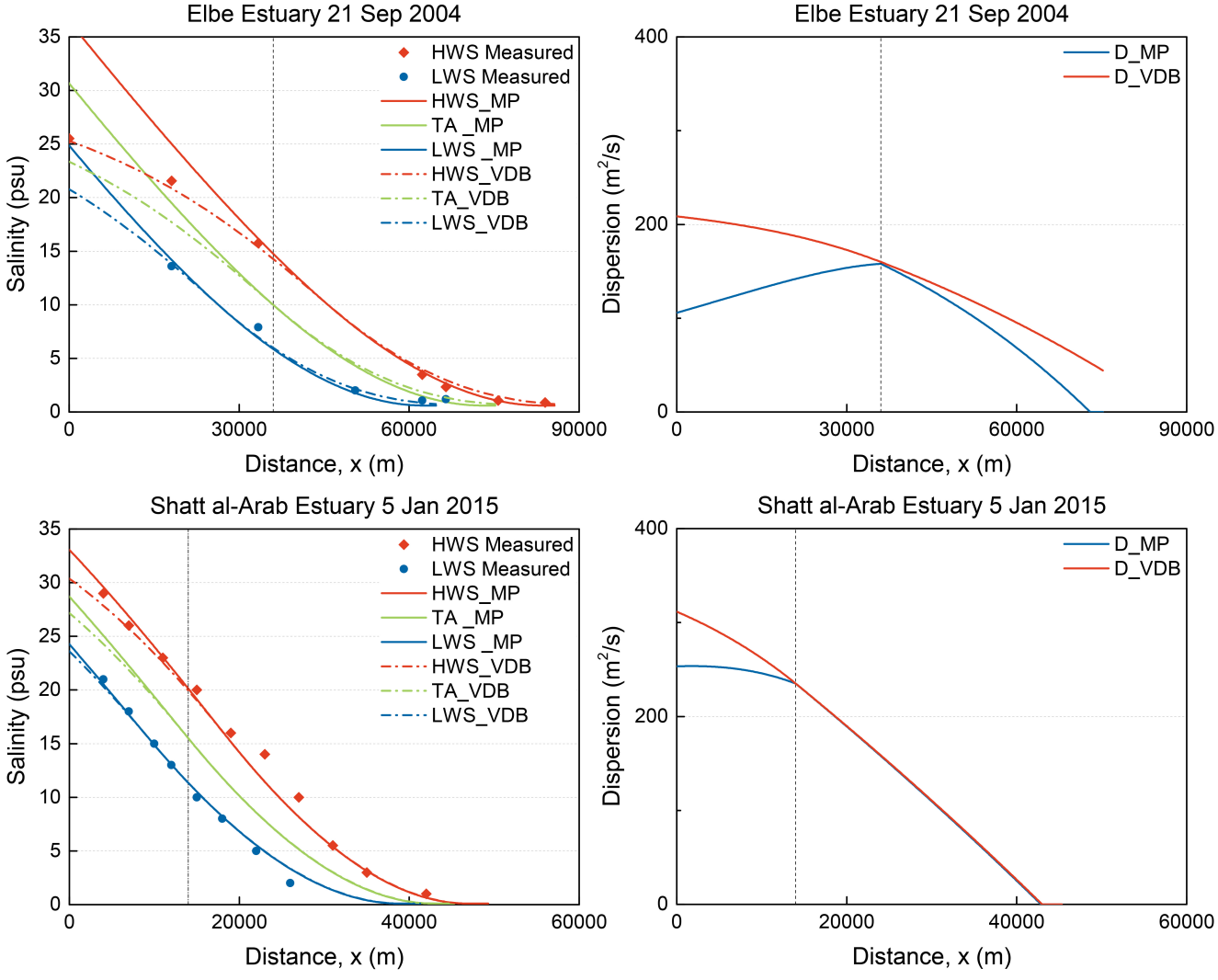

Earth Syst. Dynam. Discuss., https://doi.org/10.5194/esd-2018-78
Manuscript under review for journal Earth Syst. Dynam.
Discussion started: 3 December 2018
© Author(s) 2018. CC BY 4.0 License.

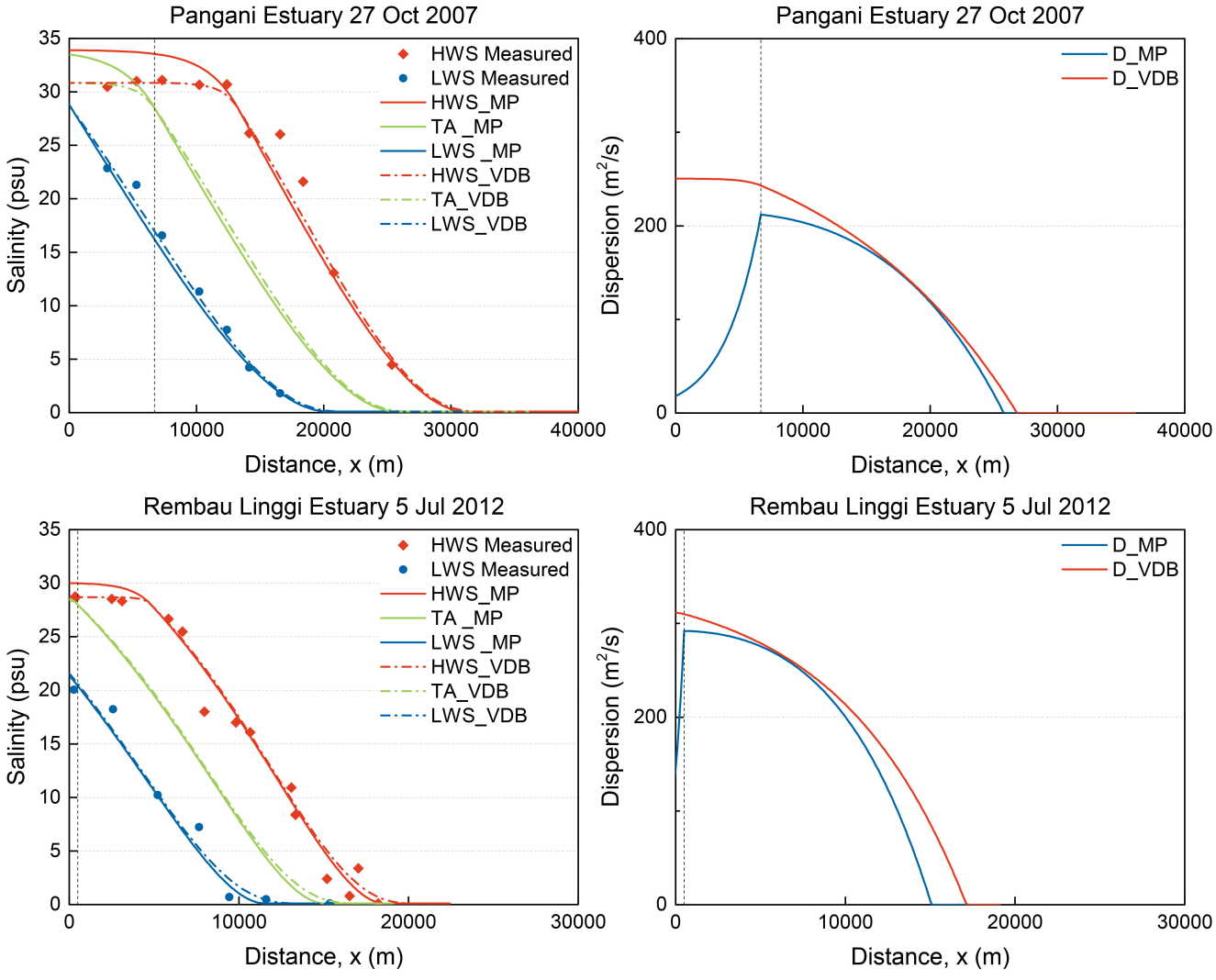

Earth Syst. Dynam. Discuss., https://doi.org/10.5194/esd-2018-78
Manuscript under review for journal Earth Syst. Dynam.
Discussion started: 3 December 2018
© Author(s) 2018. CC BY 4.0 License.

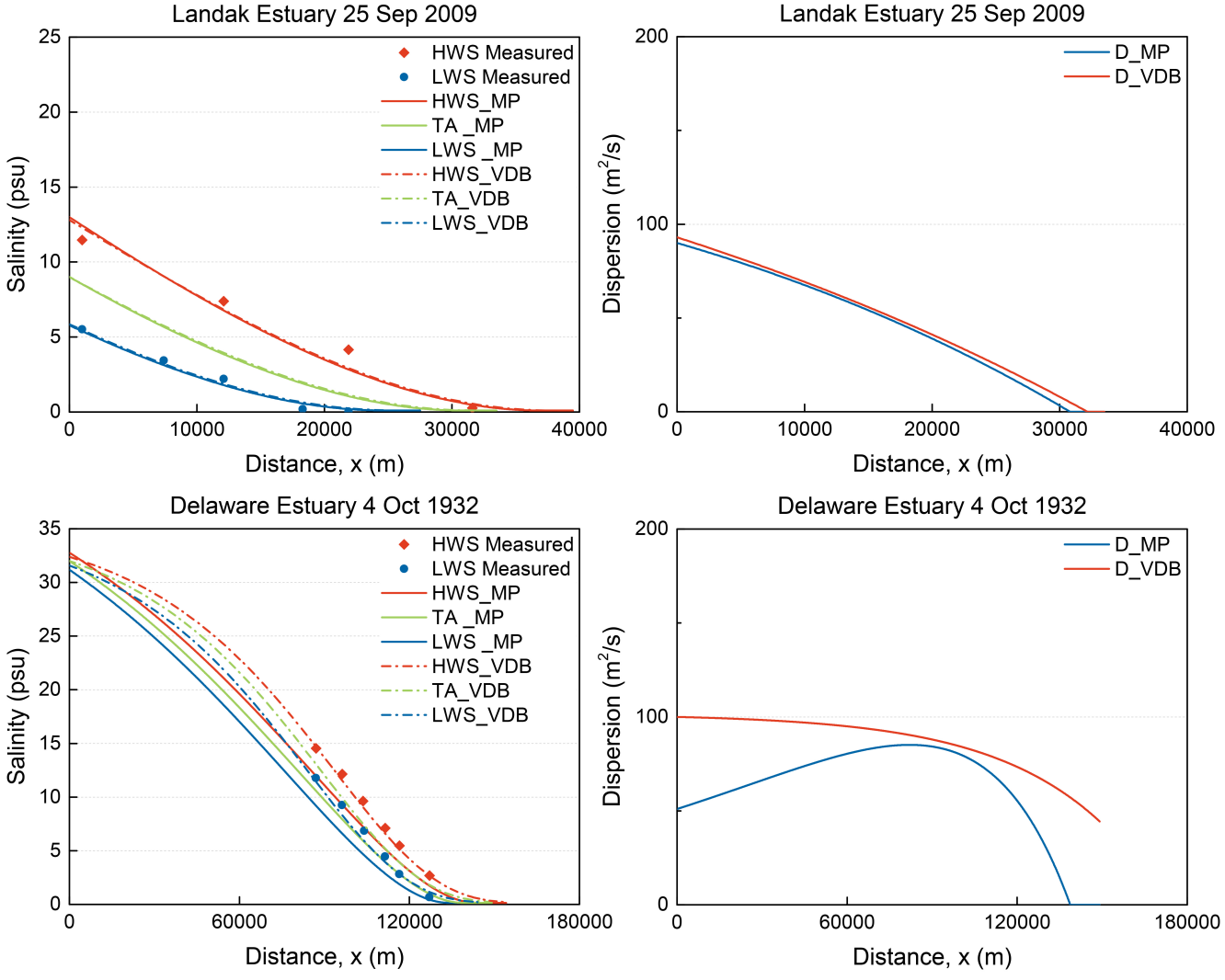

Earth Syst. Dynam. Discuss., https://doi.org/10.5194/esd-2018-78
Manuscript under review for journal Earth Syst. Dynam.
Discussion started: 3 December 2018
© Author(s) 2018. CC BY 4.0 License.

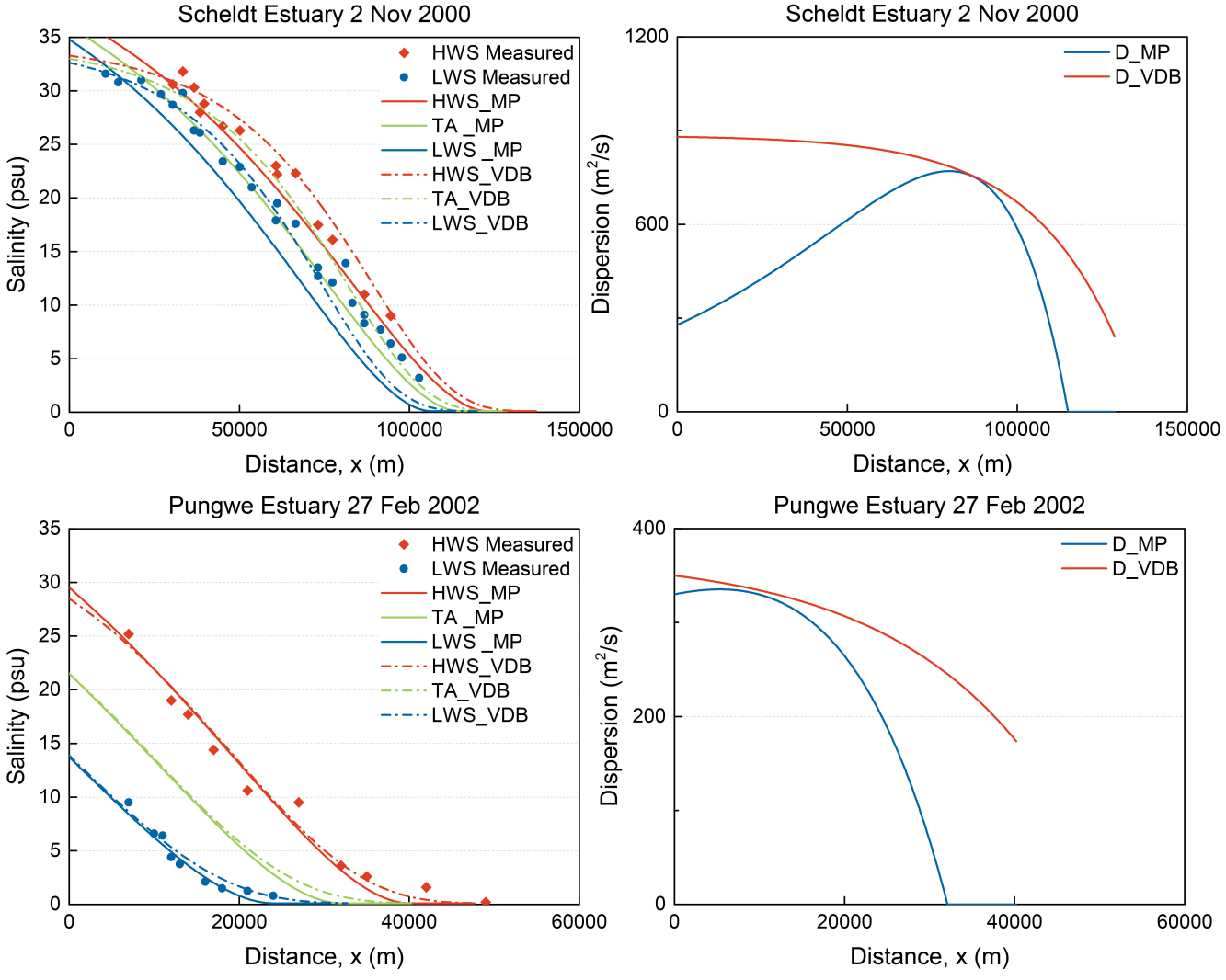

Earth Syst. Dynam. Discuss., https://doi.org/10.5194/esd-2018-78
Manuscript under review for journal Earth Syst. Dynam.
Discussion started: 3 December 2018
© Author(s) 2018. CC BY 4.0 License.

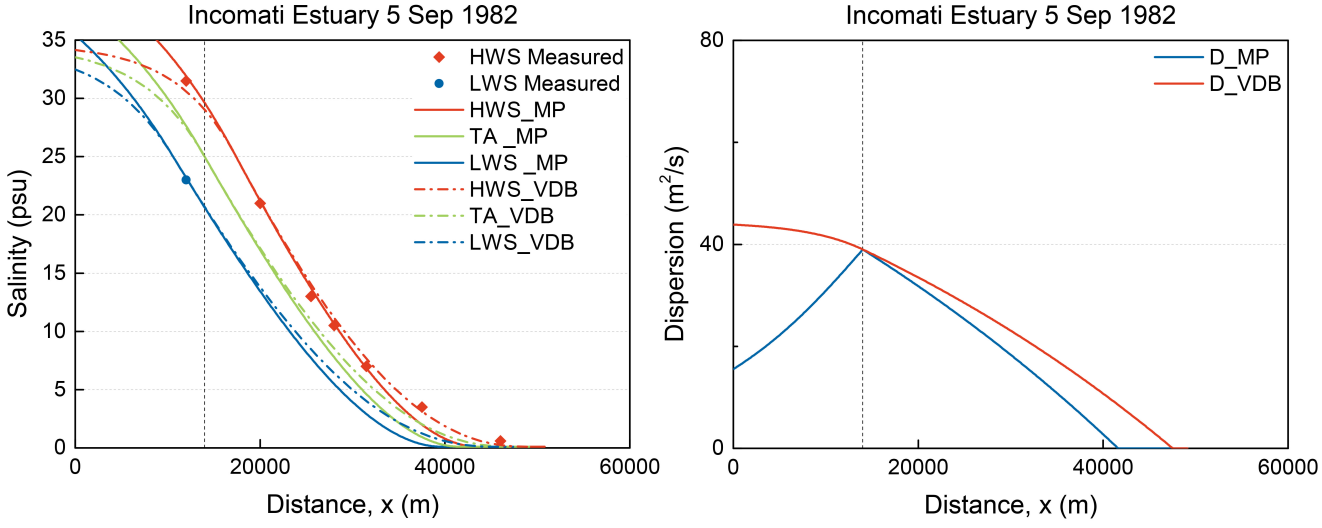

Figure B.1 Left: Application of the analytical solution from the maximum power method (solid lines) to observations (symbols) for high water slack (in red) and low water slack (in blue). The green line shows the tidal average condition. Dash dot lines reflect applications of the Van der Burgh method. Right: Simulated dispersion coefficient using different methods.

Acknowledgements. The first author is financially supported for her PhD research by the China Scholarship Council.

© Author(s) 2018. CC BY 4.0 License.

References

Fischer, H. B., List, E. J., Koh, R. C. Y., Imberger, J., and Brooks, N. H.: Mixing in inland and coastal waters, Academic Press, New York, doi:10.1016/C2009-0-22051-4, 1979.

Gisen, J. I. A.: Prediction in ungauged estuaries, Ph.D. thesis, Delft University of Technology, doi:10.4233/uuid:a4260691-15fb-4035-ba94-50a4535ef63d, 2015.

Kleidon, A.: Thermodynamic foundations of the Earth system, Cambridge University Press, London, doi:10.1017/CBO9781139342742, 2016.

Kuijper, K., and Van Rijn, L. C.: Analytical and numerical analysis of tides and salinities in estuaries; part II: salinity distributions in prismatic and convergent tidal channels, Ocean Dynam., 61(11), 1743–1765, doi:10.1007/s10236-011-0454-z, 2011.

Nguyen, A. D., Savenije, H. H. G., van der Wegen, M., and Roelvink, D.: New analytical equation for dispersion in estuaries with a distinct ebb-flood channel system, Estuar. Coast. Shelf S., 79(1), 7–16, doi:10.1016/j.ecss.2008.03.002, 2008.

Savenije, H. H. G.: Salinity and tides in alluvial estuaries, Elsevier, Amsterdam, doi:10.1016/B978-0-444-52107-1.X5000-X, 2005.

Savenije, H. H. G.: Salinity and tides in alluvial estuaries, 2ndEdn, http://salinityandtides.com/.

Zhang, Z., and Savenije, H. H. G.: The physics behind Van der Burgh's empirical equation, providing a new predictive equation for salinity intrusion in estuaries, Hydrol. Earth Syst. Sci., 21, 3287–3305, doi:10.5194/hess-21-3287-2017, 2017.

Zhang, Z., and Savenije, H. H. G.: Thermodynamics of saline and fresh water mixing in estuaries, Earth Syst. Dynam., 9, 241–247, doi:10.5194/esd-9-241-2018, 2018.

Earth Syst. Dynam. Discuss., https://doi.org/10.5194/esd-2018-78
Manuscript under review for journal Earth Syst. Dynam.
Discussion started: 3 December 2018
© Author(s) 2018. CC BY 4.0 License.

Earth System Dynamics
Discussions
Open Access
EGU

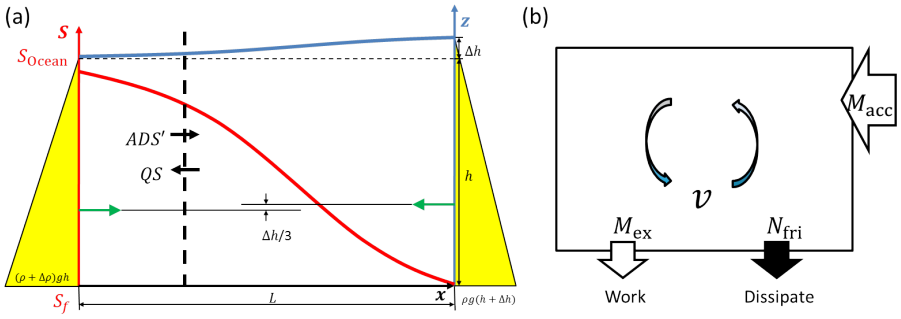

Figure 1. (a) Systematic salt transport in estuaries, with the seaside on the left and the riverside on the right. The water level (in blue) has a slope as a result of the salinity distributions (in red). The hydrostatic forces on both sides have different working lines which triggers the gravitational circulation, providing an accelerating moment M_{acc} to the system. (b) A box-model displaying the moment balance in open estuarine systems.

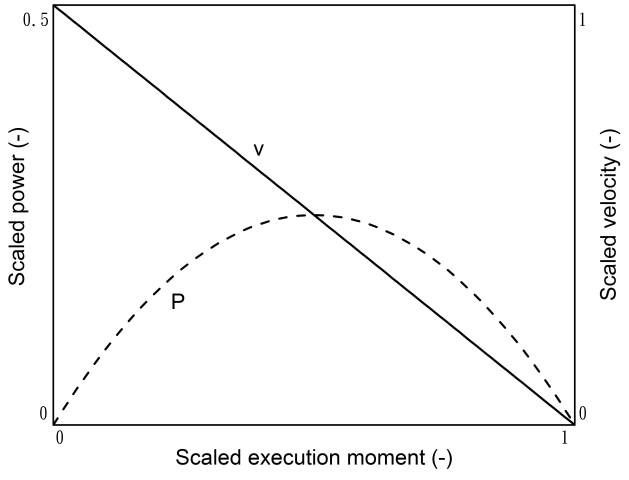

Figure 2. Sketch of the sensitivity of the exchange flow velocity v to the working moment M_{ex}.

Earth Syst. Dynam. Discuss., https://doi.org/10.5194/esd-2018-78
Manuscript under review for journal Earth Syst. Dynam.
Discussion started: 3 December 2018
© Author(s) 2018. CC BY 4.0 License.

Earth System Dynamics
Discussions
Open Access
EGU

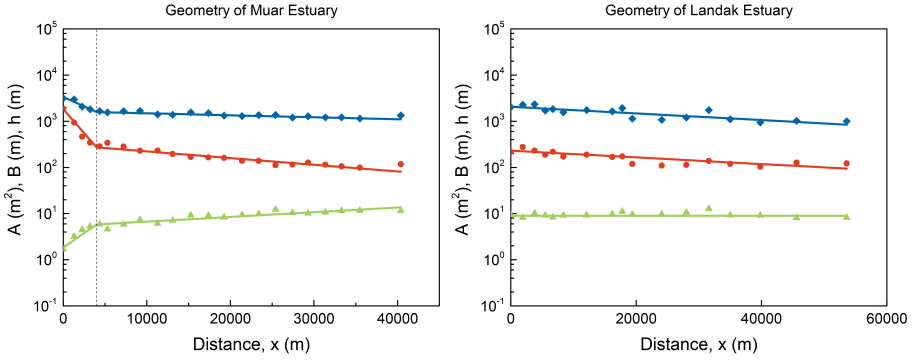

Figure 3. Semi-logarithmic presentation of estuary geometry, comparing simulated (lines) to the observations (symbols), including cross-sectional area (blue diamonds), width (red dots), and depth (green triangles).

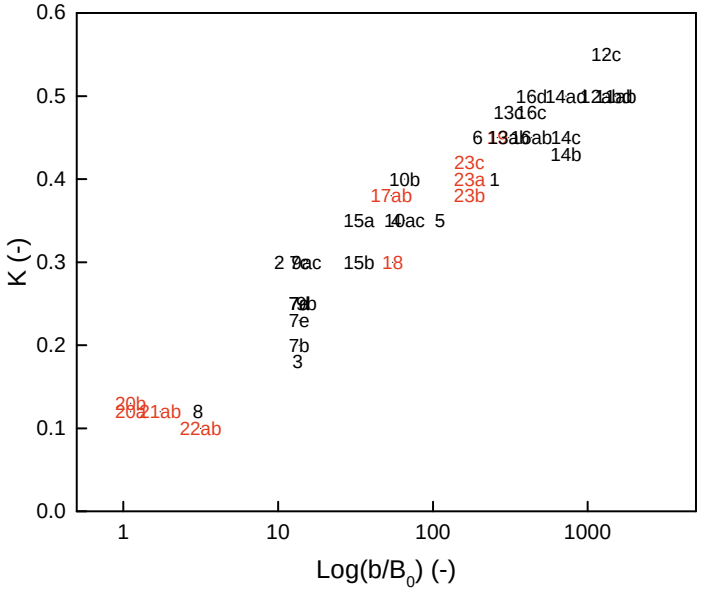

Figure 4. Comparison of the geometry to the Van der Burgh coefficient. The red color represents estuaries from a less reliable dataset.

Earth Syst. Dynam. Discuss., https://doi.org/10.5194/esd-2018-78
Manuscript under review for journal Earth Syst. Dynam.
Discussion started: 3 December 2018
© Author(s) 2018. CC BY 4.0 License.

Earth System Dynamics
Discussions
Open Access
EGU

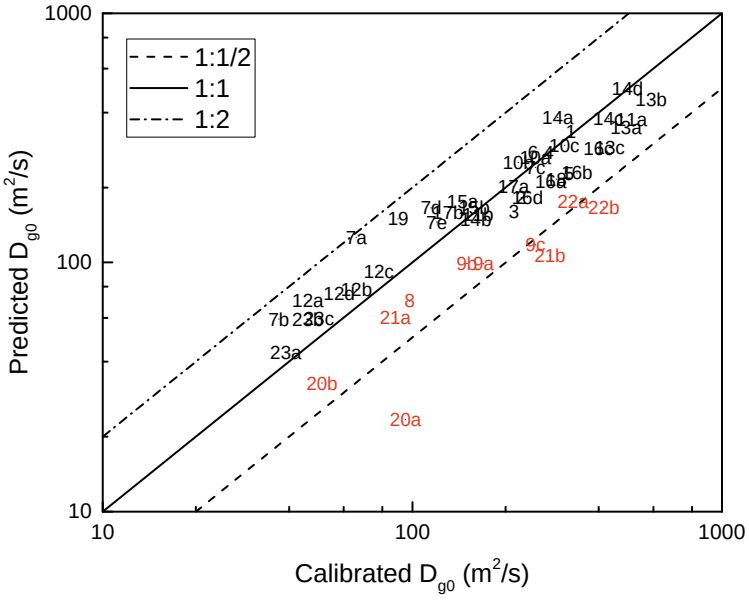

Figure 5. Comparison of calibrated and predicted D_{g0} values by using $C_3 = 6.8 \times 10^{-3}$. Labels in red indicating the estuaries have relatively poor performance are presented for validation.

Earth Syst. Dynam. Discuss., https://doi.org/10.5194/esd-2018-78
Manuscript under review for journal Earth Syst. Dynam.
Discussion started: 3 December 2018
© Author(s) 2018. CC BY 4.0 License.

Earth System Dynamics
Discussions
Open Access
EGU

Table 1. Summary of application results using two methods.

Label	S_0	Maximum power		Van der Burgh	
		D_0 (m^2/s)	C_3 ($psu^{-1}ms^{-2}$)	D_0 (m^2/s)	K (-)
1*	15	325	0.0064	325	0.4
2*	10	225	0.0082	225	0.3
3*	28	213	0.0089	255	0.18
4*	18	275	0.0066	280	0.35
5*	19	320	0.0093	330	0.35
6*	18	245	0.0059	250	0.45
7a	29	66	0.0035	68	0.25
7b	32.5	37	0.0043	42	0.2
7c*	22	250	0.0069	258	0.3
7d	25	115	0.0046	118	0.25
7e	26	120	0.0055	125	0.23
8*	31	98	0.0093	245	0.12
9a	14	170	0.0114	170	0.3
9b	12	150	0.0100	150	0.25
9c*	10	250	0.0141	250	0.3
10a	8	250	0.0063	250	0.35
10b	6.5	220	0.0058	220	0.4
10c*	13	310	0.0070	310	0.35
11a	24	510	0.0090	520	0.5
11b*	26	163	0.0069	165	0.5
12a	23	46	0.0044	51	0.5
12b	13	66	0.0056	70	0.5
12c	16	78	0.0056	92	0.55
12d*	17.5	58	0.0051	63	0.5
13a	23	490	0.0094	490	0.45
13b	25.5	590	0.0087	600	0.45
13c*	16.5	435	0.0099	440	0.48
14a	11	295	0.0051	305	0.5
14b	1	160	0.0071	165	0.43
14c*	8.5	430	0.0076	430	0.45

continued on next page

Earth Syst. Dynam. Discuss., https://doi.org/10.5194/esd-2018-78
Manuscript under review for journal Earth Syst. Dynam.
Discussion started: 3 December 2018
© Author(s) 2018. CC BY 4.0 License.

continued from previous page

Label	S_0	Maximum power		Van der Burgh	
		D_0 (m^2/s)	C_3 ($psu^{-1}ms^{-2}$)	D_0 (m^2/s)	K (-)
14d	12	495	0.0066	510	0.5
15a	10	145	0.0055	150	0.35
15b*	10	158	0.0063	160	0.3
16a	11.5	280	0.0088	280	0.45
16b	16	340	0.0099	340	0.45
16c	27	400	0.0092	400	0.48
16d*	15.5	235	0.0086	235	0.5
17a*	28.5	212	0.0070	243	0.38
17b	28	130	0.0054	145	0.38
18*	28	292	0.0090	310	0.3
19*	9	90	0.0040	93	0.45
20a	11	95	0.0269	200	0.12
20b*	32	51	0.0103	100	0.13
21a	31	88	0.0097	225	0.12
21b*	33	278	0.0173	800	0.12
22a*	21.5	330	0.0124	350	0.1
22b	20	415	0.0165	500	0.1
23a*	25	39	0.0058	39	0.4
23b	17	46	0.0052	46	0.38
23c	16	50	0.0056	50	0.42